INTERNATIONAL JOURNAL FOR NUMERICAL METHODS IN FLUIDS, VOL. 16, 931–948 (1993)

EVALUATION OF VARIOUS HIGH-ORDER-ACCURACY SCHEMES WITH AND WITHOUT FLUX LIMITERS

PANOS TAMAMIDIS AND DENNIS N. ASSANIS

Department of Mechanical and Industrial Engineering, University of Illinois at Urbana-Champaign, 1206 West Green Street, Urbana, Illinois 61801, U.S.A.

SUMMARY

Conventional high-order schemes with reduced levels of numerical diffusion produce results with spurious oscillations in areas where steep velocity gradients exist. To prevent the development of non-physical oscillations in the solution, several monotonic schemes have been proposed. In this work, three monotonic schemes, namely Van Leer's scheme, Roe's flux limiter and the third-order SHARP scheme, are compared and evaluated against schemes without flux limiters. The latter schemes include the standard first-order upwind scheme, the second-order upwind scheme and the QUICK scheme. All the above schemes are applied to four two-dimensional problems: (i) rotation of a scalar 'cone' field, (ii) transport of a scalar 'square' field, (iii) mixing of a cold with a hot front and (iv) deformation of a scalar 'cone' field. These problems test the ability of the selected schemes to produce oscillation-free and accurate results in critical convective situations. The evaluation of the schemes is based on several aspects, such as accuracy, economy and complexity. The tests performed in this work reveal the merits and demerits of each scheme. It is concluded that high-order schemes with flux limiters can significantly improve the accuracy of the results.

KEY WORDS High-order schemes Flux limiters Numerical diffusion Unsteady flows Monotonicity Finite differences

INTRODUCTION

Satisfactory numerical modelling of convection presents a well-known dilemma to the CFD engineer. On the one hand, high-order accuracy schemes may lead to unphysical, oscillatory behaviour in regions where steep gradients exist. On the other hand, computations based on the classical first-order upwind scheme or other low-order schemes[1–4] often suffer from severe inaccuracies due to truncation error. Although, in principle, grid refinement can alleviate this latter problem, the necessary degree of refinement is often impracticable for engineering purposes,[5] especially if one is attempting to model three-dimensional turbulent flows.

Higher-order upwind schemes have been successful in eliminating artificial diffusion while minimizing numerical dispersion. In the case of second-order upwinding[6] the leading truncation error is a third-order derivative term, which could potentially cause oscillations in the solution. The quadratic upwind-biased scheme of Leonard,[7] known as QUICK (Quadratic Upstream Interpolation for Convective Kinematics), has a fourth-order derivative (which is dissipative) as the leading truncation error term. However, higher-order dispersion terms may still cause overshoots and undershoots in areas where steep gradients of the convected variable exist.

An early attempt towards developing a high-order monotonic scheme was made by Borris and Book,[8] who proposed the Flux-Corrected Transport (FCT) scheme. In their procedure, a low-

0271–2091/93/100931–18$14.00

Received 27 August 1992
Revised 15 December 1992

resolution solution is first obtained using a low-order accurate scheme. This initial solution is then corrected by adding high-order terms which are limited in order to produce monotonic results. Although this sophisticated procedure was later enhanced by Zalesak,[9] it is still quite complicated and demanding in computer time.[10] In his search for the ultimate conservative scheme, Van Leer[11] developed the Monotonic Piecewise Linear (MPL) scheme. In this second-order scheme, which is based on zone averages instead of mesh point values, monotonicity is enforced by suitably adjusting the second-order terms. Based on Van Leer's method, Collela and Woodwork[12] developed a third-order method using Piecewise Parabolic Monotonic (PPM) functions.

Another class of monotonic schemes has been developed by Roe[13,14] and extended by Chakravarthy and Osher.[15] These schemes are based on approximate Riemann solutions and have been originally developed for the prediction of inviscid compressible flows with strong shocks. Similar schemes include the high-resolution schemes of Harten,[16] the ENO (Essentially Non-Oscillatory) schemes of Shu and Osher,[17,18] the slope modification method of Yang[19] and the TVD scheme of Wang and Widhopf,[20] to name a few. A new generation of multidimensional monotonic convective schemes, based on non-linear characteristics in the normalized variable diagram, has been proposed by Leonard.[21] The new scheme, named SHARP (Simple High-Accuracy Resolution Program) is a monotonic version of his earlier QUICK scheme. Similar to SHARP is the simpler SMART scheme,[22] which is based on piecewise linear characteristics.

While Sweby[23] compared Van Leer's,[11] Roe's,[13,14] and Chakravarthy and Osher's[15] schemes in several one-dimensional flows, a comprehensive evaluation of various high-order-accuracy schemes, with and without flux limiters, in a range of two-dimensional unsteady flows, has not been reported in the literature. The goal of the present work is to compare and assess the performance of three promising monotonic schemes, namely Van Leer's MPL scheme,[11] Roe's flux limiter[14] and Leonard's SHARP scheme,[21] against three widely used schemes without flux limiters. The latter schemes include the classical First-Order Upwind scheme (FOU), the Second-Order Upwind scheme (SOU)[6] and the QUICK scheme.[7]

Four two-dimensional benchmark problems are used to test the various schemes in different situations: (i) rotation of a scalar 'cone' field, (ii) transport of a scalar 'square' field, (iii) mixing of a cold with a hot front and (iv) deformation of a scalar 'cone' field. The first two problems test the ability of the schemes to produce oscillation-free and accurate results in critical convective situations. The third problem is less severe, thus allowing for a more realistic comparison of the schemes. The final test problem is very severe and fully tests the ability of the schemes to produce results without unphysical overshoots and oscillations. The evaluation of the schemes is based on several aspects, such as accuracy, economy and complexity. The tests performed in this work reveal the merits and demerits of proposed schemes for discretizing convective terms in linear problems.

MATHEMATICAL FORMULATION

Problem definition

The class of problems considered in this work is the transport of a scalar field in the absence of any other physical phenomena except convection, e.g. transport of a non-diffusive tracer (Figure 1). Assuming a given flow field, the governing equation in two-dimensional space is

$$\frac{\partial q}{\partial t}+u\frac{\partial q}{\partial x}+v\frac{\partial q}{\partial y}=0, \tag{1}$$

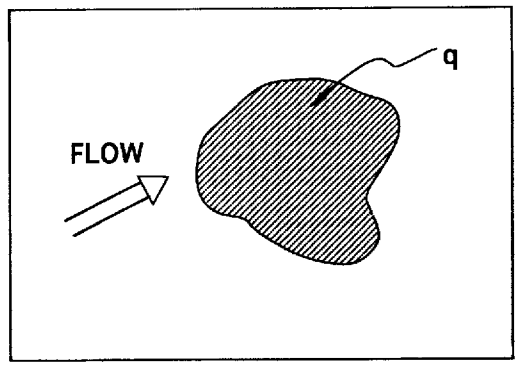

Figure 1. Problem definition

where q is the scalar, and u and v are the two velocity components. After some manipulations, this linear equation can be written in the following form:

$$\frac{\partial q}{\partial t}+\frac{\partial (uq)}{\partial x}+\frac{\partial (vq)}{\partial y}=q\left(\frac{\partial u}{\partial x}+\frac{\partial v}{\partial y}\right). \tag{2}$$

The boundary conditions considered throughout this work are zero gradients of the variable q along each boundary. Note that for divergence-free flow fields, the RHS of equation (2) vanishes.

Equation (2) is ideal for examining the performance of various schemes for discretizing convective terms, since it describes problems with pure convection. Thus, this paper deals with solutions of equation (2) in different flow conditions and with various initial conditions for the scalar q.

Numerical procedure

Equation (2) is solved using the standard finite volume method. Therefore, by integrating equation (2) over a finite volume we obtain

$$\iint \frac{\partial q}{\partial t}\,dx\,dy=-\iint \frac{\partial (uq)}{\partial x}\,dx\,dy-\iint \frac{\partial (vq)}{\partial y}\,dx\,dy+\iint q\left(\frac{\partial u}{\partial x}+\frac{\partial v}{\partial y}\right)dx\,dy. \tag{3}$$

The integral on the LHS of equation (3) is calculated by assuming a uniform value of q over the control volume. Also, for the calculation of the integrals on the RHS we assume uniform fluxes along each cell face. Then, for a constant grid spacing in each direction we obtain

$$\begin{aligned}\frac{\partial q_{ij}}{\partial t}\Delta x\,\Delta y=&-[(uq)_{i+1/2,j}-(uq)_{i-1/2,j}]\Delta y-[(vq)_{i,j+1/2}-(vq)_{i,j-1/2}]\Delta x\\&+q[(u_{i+1/2,j}-u_{i-1/2,j})\Delta y+(v_{i,j+1/2}-v_{i,j-1/2})\Delta x].\end{aligned} \tag{4}$$

Integrating equation (4) in time and using a simple explicit formulation, we obtain

$$\begin{aligned}q_{ij}^{n+1}=&q_{ij}^{n}-[F_{i+1/2,j}-F_{i-1/2,j}]^{n}\frac{\Delta t}{\Delta x}-[F_{i,j+1/2}-F_{i,j-1/2}]^{n}\frac{\Delta t}{\Delta y}\\&-q_{ij}^{n}\left[(u_{i+1/2,j}-u_{i-1/2,j})^{n}\frac{\Delta t}{\Delta x}+(v_{i,j+1/2}-v_{i,j-1/2})^{n}\frac{\Delta t}{\Delta y}\right],\end{aligned} \tag{5}$$

where F is the flux of q, Δt is the time step, and the superscript n denotes values at the previous time step. Note that this simple explicit temporal scheme could potentially affect the performance of any spatial discretization scheme in time-dependent problems. In the latter, accuracy does not only depend on the spatial formulation but also on the manner in which the rate of change term is represented. Since this work is addressing the evaluation of alternative spatial discretization schemes, low Courant numbers have been maintained in all test cases to minimize the impact of the choice of time discretization scheme.

DIFFERENCING SCHEMES

Schemes without flux limiters

First-order upwind scheme (FOU). This scheme assumes the 'upwind' values of q at a cell face. At the east cell face, for example, the flux is calculated as follows:

$$F_{i+1/2,j}=\frac{(u_{i+1/2,j}+|u_{i+1/2,j}|)}{2}q_{i,j}+\frac{(u_{i+1/2,j}-|u_{i+1/2,j}|)}{2}q_{i+1,j}, \tag{6}$$

where the superscript n has been omitted for notation convenience. Note that when $u_{i+1/2,j}$ is positive, the second term becomes zero, and the value of $q_{i,j}$ is used. In the opposite case, i.e. when $u_{i+1/2,j}$ is negative, the value of $q_{i+1,j}$ is used. Thus, this scheme is called upwind.

The upwind scheme has two advantages which have made it the most widely used scheme: (i) it produces stable and oscillation-free solutions and (ii) it is very easy to implement in a code. However, it has a serious drawback. The omitted leading term in equation (6) is of the type $\partial^2 u/\partial x^2$, which represents diffusion. In many flow conditions, and especially in high-Re flows, this omitted diffusion-like term becomes large and degrades the accuracy of the results. Although the accuracy of the results can be improved by increasing the resolution of the grid, this may be impractical for three-dimensional applications.

Second-order upwind scheme (SOU). The accuracy of the classical first-order upwind scheme can be improved by retaining in the calculations the second-order derivatives which were omitted in eqaution (6). The resulting SOU scheme[6] is considerably more accurate than the FOU scheme. The flux terms are now formed as follows:

$$F_{i+1/2,j}=\frac{(u_{i+1/2,j}+|u_{i+1/2,j}|)}{2}(\tfrac{3}{2}q_{i,j}-\tfrac{1}{2}q_{i-1,j})+\frac{(u_{i+1/2,j}-|u_{i+1/2,j}|)}{2}(\tfrac{3}{2}q_{i+1,j}-\tfrac{1}{2}q_{i+2,j}). \tag{7}$$

The SOU scheme is somewhat more complex than the FOU scheme, since it uses a four-point stencil for calculating the fluxes. However, it is also more accurate, since the leading truncation error in equation (7) is a third-order derivative term; thus, the SOU scheme introduces less artificial diffusion in the solution. Unfortunately, this third-order derivative term can potentially cause oscillations in the solution, especially when discontinuous gradients of the variable q exist.

Quadratic upstream-biased scheme (QUICK). The QUICK scheme[7] is a third-order upwind scheme. This scheme is upwind-biased, since it calculates fluxes using information not only from the upstream nodes but also from the first downstream node. At the east cell face, for example, the flux is formed as follows:

$$\begin{aligned}F_{i+1/2,j}=&\frac{(u_{i+1/2,j}+|u_{i+1/2,j}|)}{2}[\tfrac{1}{2}(q_{i+1,j}+q_{i,j})-\tfrac{1}{8}\mathrm{CURVX}_{i,j}]\\&+\frac{(u_{i+1/2,j}-|u_{i+1/2,j}|)}{2}[\tfrac{1}{2}(q_{i+1,j}+q_{i,j})-\tfrac{1}{8}\mathrm{CURVX}_{i+1,j}],\end{aligned} \tag{8}$$

where CURVX is the curvature term given by

$$\text{CURVX}_{i,j}=q_{i+1,j}-2q_{i,j}+q_{i-1,j}. \tag{9}$$

The QUICK scheme is of the same order of complexity as the SOU scheme, since it also uses a four-point stencil for calculating the fluxes. However, increased accuracy is achieved by making the QUICK scheme upwind-biased instead of fully upwind, as in the SOU scheme. The leading truncation term in equation (8) is a fourth-order derivative term, which is much less dissipative than the second-order dissipation term in the FOU scheme.

Schemes with flux limiters

Van Leer's scheme (MPL). Van Leer's[11] MPL scheme is based on zone averages instead of grid point values, which is the case with the previous schemes. Assuming a piecewise linear distribution of the scalar q inside a zone, i.e.

$$q_i(x)=q_i+x\,\overline{\Delta q_i}, \tag{10}$$

where overbars denote zone-averaged values, and positive u-velocity at the east cell face, the flux can be expressed as

$$F_{i+1/2,j}=|u_{i+1/2,j}|\left[q_{i,j}+\tfrac{1}{2}\overline{\Delta q}_{ij}\left(\frac{\Delta x}{\Delta t}-|u_{i+1/2,j}|\right)\right], \tag{11}$$

where $\overline{\Delta q}_{ij}=(1/2)\,(q_{i+1,j}-q_{i-1,j})$. When $u_{i+1/2,j}$ is negative, the flux is calculated using information from the $i+1$ zone:

$$F_{i+1/2,j}=|u_{i+1/2,j}|\left[-q_{i+1,j}+\tfrac{1}{2}\overline{\Delta q}_{i+1,j}\left(\frac{\Delta x}{\Delta t}-|u_{i+1/2,j}|\right)\right]. \tag{12}$$

Van Leer introduced the idea of monotonicity by limiting the function in equation (10) to the values inside the range spanned by the neighbouring mesh averages, i.e

$$q_{i+1/2,j}=q_{i,j}+\tfrac{1}{2}\overline{\Delta q}_{i,j}\leqslant q_{i+1,j} \tag{13}$$

and

$$q_{i+1/2,j}=q_{i,j}+\tfrac{1}{2}\overline{\Delta q}_{i,j}\geqslant q_{i,j}, \tag{14}$$

where q has been assumed to increase monotonically. Similar relations can be derived when q decreases monotonically. To prevent the introduction of new extrema in the solution, Van Leer's scheme limits the value of $\overline{\Delta q}$ to zero when q is not varying monotonically. These checks ensure oscillation-free solutions. The overall algorithm is second-order-accurate.

Monotonic second-order upwind scheme (MSOU). Roe[13,14] developed a second-order monotonic scheme, which is based on an approximate Riemann solver. His original formulation is presented in incremental or fluctuation format rather than the classical numerical flux formulation. Sweby[18] converted Roe's transfer function to a flux limiter. Thus, the SOU scheme can be made monotonic following Sweby's procedure. The resulting monotonic second-order upwind (MSOU) scheme is fully upwind. The numerical fluxes are written in the following format:

$$F_{i+1/2,j}=\frac{(u_{i+1/2,j}+|u_{i+1/2,j}|)}{2}(q_{i,j}+\tfrac{1}{2}\varphi_{ij}^{-}\,\Delta q_{ij}^{-})+\frac{(u_{i+1/2,j}-|u_{i+1/2,j}|)}{2}(q_{i+1,j}-\tfrac{1}{2}\varphi_{ij}^{+}\,\Delta q_{ij}^{+}), \tag{15}$$

where

$$\Delta q_{ij}^{-} = q_i - q_{i-1}, \tag{16}$$

$$\Delta q_{ij}^{+} = q_{i+2} - q_{i+1}, \tag{17}$$

$$\varphi_{ij}^{\mp} = \max\{0, \min(2r_{ij}^{\mp}, 1), \min(r_{ij}^{\mp}, 2)\}, \tag{18}$$

$$r_{ij}^{-} = \frac{(q_{i+1,j} - q_{i,j})}{(q_{i,j} - q_{i-1,j})}, \tag{19}$$

$$r_{ij}^{+} = \frac{(q_{i,j} - q_{i+1,j})}{(q_{i+1,j} - q_{i+2,j})}, \tag{20}$$

where r_{ij} is the ratio of consecutive gradients, and φ_{ij} is the flux limiter which corresponds to Roe's[14] 'superbee' compressive transfer function. The resulting scheme is monotonic and does not allow the appearance of non-physical oscillations.

SHARP scheme. Leonard[21] has presented a monotonic version of his earlier QUICK scheme. The new scheme, named SHARP, retains QUICK's third-order accuracy. SHARP represents a new generation of multidimensional monotonic convective schemes based on non-linear characteristics in the so-called normalized variable diagram.[21] In the SHARP scheme, the calculation of fluxes is based on the following formulation:

$$F_{i+1/2,j} = u_{i+1/2,j}(q_{i,j} + \tfrac{1}{2}\mathrm{CF}\,\mathrm{CURV}_{ij}), \tag{21}$$

where

$$\mathrm{CURV}_{ij} = (q_{i+2,j} - q_{i+1,j} - q_{i,j} + q_{i-1,j}) - \mathrm{sign}(u_{i+1/2,j})(q_{i+2,j} - 3q_{i+1,j} + 3q_{i,j} - q_{i-1,j}), \tag{22}$$

where CF is the curvature factor, being equal to 1/8 in the case of the QUICK scheme. This formulation automatically takes into account the direction of the velocity.

The monotonicity is imposed by limiting the curvature factor. The algorithm begins by computing $|q_d - q_u|$ and going immediately to QUICK if this absolute value is less than 10^{-5}. If not, the curvature factor is calculated as follows:

for $\tilde{q}_c \leqslant -1$: $\mathrm{CF} = 0{\cdot}125$, (23a)

for $-1 < \tilde{q}_c \leqslant 0$: $\mathrm{CF} = (0{\cdot}5 + 0{\cdot}125\tilde{q}_c)/(1 - 2\tilde{q}_c)$, (23b)

for $0 < \tilde{q}_c < 0{\cdot}3$: $\mathrm{CF} = [\tilde{q}_c^2 - (1 + \tilde{q}_c)(\tilde{q}_c - 0{\cdot}5) - \tilde{q}_c^{1/2}(1 - \tilde{q}_c)^{3/2}]/(1 - 2\tilde{q}_c)^2$, (23c)

for $0{\cdot}3 \leqslant \tilde{q}_c \leqslant 0{\cdot}7$: $\mathrm{CF} = 0{\cdot}125 - 0{\cdot}2609(\tilde{q}_c - 1{\cdot}5) + 0{\cdot}13613(\tilde{q}_c - 0{\cdot}5)^2$, (23d)

for $0{\cdot}7 < \tilde{q}_c < 1$: $\mathrm{CF} = [\tilde{q}_c^2 - (1 + \tilde{q}_c)(\tilde{q}_c - 0{\cdot}5) - \tilde{q}_c^{1/2}(1 - \tilde{q}_c)^{3/2}]/(1 - 2\tilde{q}_c)^2$, (23e)

for $1 \leqslant \tilde{q}_c < 1{\cdot}5$: $\mathrm{CF} = (\tilde{q}_c - 1)/(4\tilde{q}_c - 2)$, (23f)

for $1{\cdot}5 \leqslant \tilde{q}_c$: $\mathrm{CF} = 0{\cdot}125$, (23g)

where $\tilde{q}_c$, the normalized variable at point (i, j), is defined by

$$\tilde{q}_c = \frac{q_c - q_u}{q_d - q_u} \tag{24}$$

and the subscripts u, c and d denote the upstream, central and downstream nodes, respectively. The above formulation can be programmed using Block-IF statements. For scalar machines it does not require considerably more computer time than any standard formulation. However, in

vector architectures such as the one of the Cray-Y/MP supercomputer, the above Block-IF statements cause vectorization difficulties. While the current version 5·0 of the cft77 compiler on the Cray systems can vectorize Block-IF statements, the resulting code modules are not fully optimized.

EXAMPLES

Rotation of a cone-shaped scalar field

A very good test for the various schemes is the rotation of a cone-shaped scalar field used in several studies.[10,24–27] In this test, a scalar 'cone' field is advected around by a stationary (in time) velocity field. The scalar field is named so because, when the field value is plotted in the third dimension, it appears as an inverted cone. The size of the domain is 1 unit by 1 unit and the angular velocity $\omega = 2{\cdot}0$ units. The two-dimensional (2D) schematic of the problem is shown in Figure 2(a); a 3D perspective view of the initial cone field is plotted in Figure 2(b). The maximum and minimum values of the field were $q_{\max} = 10$ and $q_{\min} = 0$, respectively. The maximum Courant number was approximately equal to 0·1, and one full rotation around the centre of the domain corresponded to 3140 iterations (i.e. time steps) on a 64×64 grid.

The results obtained after one revolution are summarized in Table I. Two grids have been used, a coarse one (32×32) and a fine one (64×64). Three parameters are tabulated: (i) the maximum field value, (ii) the minimum field value and (iii) the RMS error, defined as follows:

$$\mathrm{RMS} = \frac{\sqrt{[\sum_{ij}(q_{i,j\,\mathrm{predicted}} - q_{i,j\,\mathrm{exact}})^2]}}{\text{number of nodes}}. \tag{25}$$

The minimum and maximum values show how well each scheme is capturing the steep gradients which exist in the scalar field. The RMS error, on the other hand, reflects the overall performance of each scheme. Useful conclusions can be drawn by simultaneously examining Table I and Figures 3(a)–3(*f*), where the solution from each scheme is plotted. It is immediately noticed that

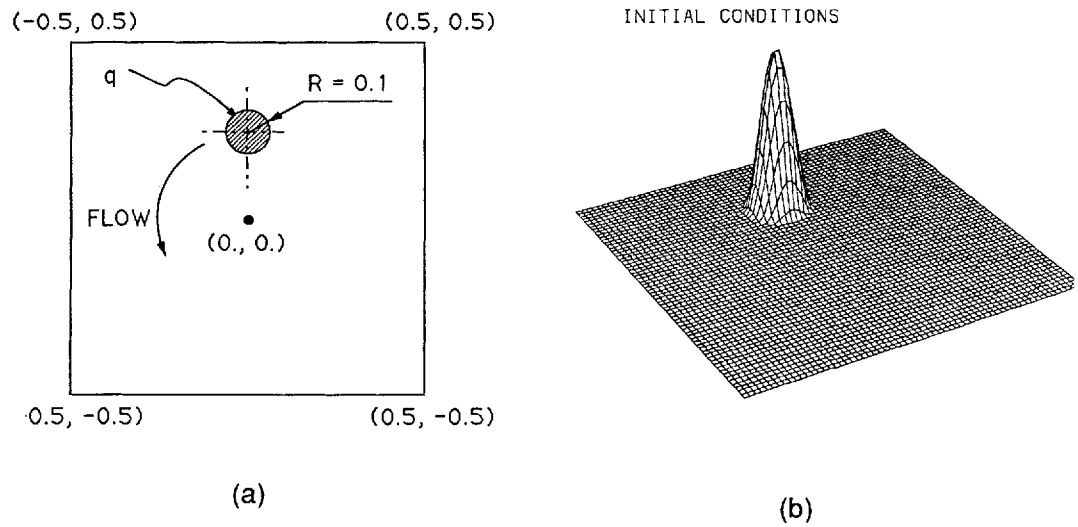

Figure 2. (a) Two-dimensional schematic of the solid-body rotation test and (b) three-dimensional perspective of the initial scalar field

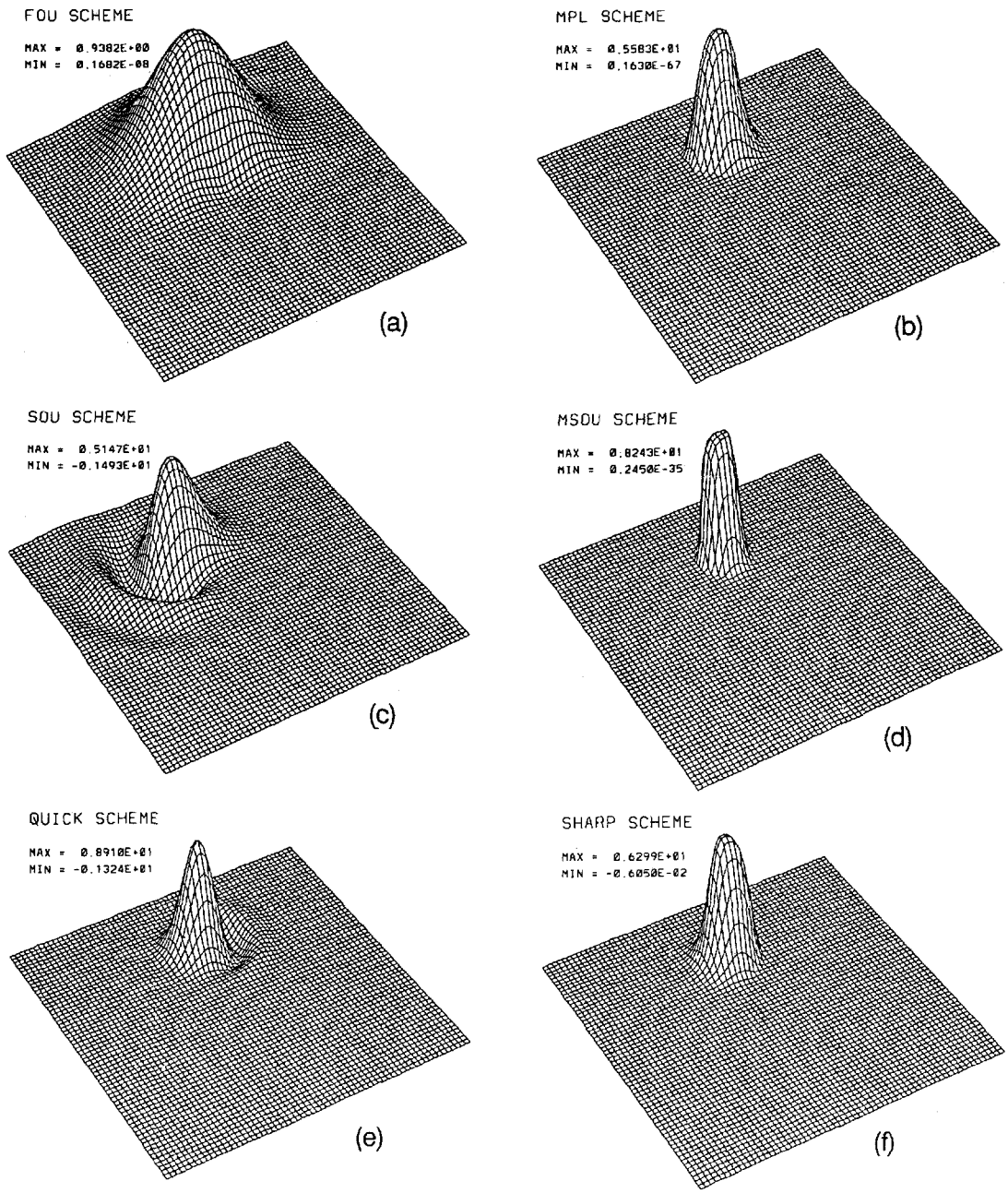

Figure 3(a)–(f). Three-dimensional perspective plots of the scalar fields in the solid-body rotation test

the solution from the FOU scheme is extremely inaccurate. The other non-monotonic schemes, i.e. SOU and QUICK, produce results with strong oscillations. Nevertheless, the specific pattern of the oscillations is quite different between the SOU and the QUICK schemes. In the former scheme, the oscillations are leading the cone, while for the latter scheme the oscillations are

Table I. Performance of the various discretization schemes in the solid-body rotation test

Scheme	32 × 32 grid			64 × 64 grid		
	Max.	Min.	RMS error	Max.	Min.	RMS error
FOU	0·477	0·000	0·672	0·938	0·000	0·642
SOU	0·831	−0·030	0·642	1·673	−0·027	0·581
QUICK	4·284	−0·751	0·472	8·910	−1·324	0·261
MPL	2·410	0·000	0·505	5·583	0·000	0·263
MSOU	3·356	0·000	0·421	8·242	0·000	0·110
SHARP	2·595	−0·002	0·497	6·300	−0·006	0·215

forming a 'wake' region just behind the cone. Also, the amplitude of the oscillations produced by QUICK is larger than the one produced by SOU.

On the other hand, the flux-limiting schemes, namely MPL, MSOU and SHARP, dramatically improve results compared to the schemes without flux limiters. Clearly, MSOU captures the maximum value of the field more closely than the other schemes. Next in ranking is Leonard's SHARP scheme, followed by the MPL scheme. The RMS error produced by MSOU on the coarse grid is approximately 20% smaller than the ones produced by MPL and SHARP. On the fine grid, the solution predicted from MSOU has 139 and 95% smaller RMS errors than MPL and SHARP, respectively. It should be noted here that SHARP introduced a minimum value of very small, negative magnitude. This could potentially cause problems if the advected variable has to be physically positive. Thus, SHARP is not strongly monotonic, but it is rather weakly monotonic. In contrast, MSOU and MPL did not introduce any negative or positive minima in the solution. The results clearly indicate that the MSOU scheme is to be preferred in this benchmark problem.

Advection of a square-shaped scalar field

The next test case is the advection of a square-shaped scalar field. It is selected because it presents an increased number of discontinuities from the previous example. According to Amsden *et al.*,[28] this test is so severe that it may even exaggerate many of the shortcomings of the various schemes. In this test, a scalar square field is advected by a fixed (with time) uniform velocity field, directed at a 45° angle with respect to the mesh directions. The domain space is 6 × 6 units, while the size of the square field is 1·5 × 1·5 units. The 2D schematic of the domain is shown in Figure 4(a) and a 3D perspective view of the initial square field is plotted in Figure 4(b). The maximum and minimum values of the field were $q_{max} = 10$ and $q_{min} = 0$, respectively. The field was advected for a length equal to 3·95 units from its initial location to the opposite corner of the domain. The u and v velocities were both equal to 1 unit. The Courant number was approximately equal to 0·19. The required time for this transport was equivalent to 140 time steps on a 40 × 40 grid.

Results for two grids of 40 × 40 and 80 × 80 cells are presented in Table II. Three parameters are reported: (i) the maximum field value, (ii) the minimum field value and (iii) the RMS error. Figures 5(a)–5(f) show 3D perspective plots of the scalar field obtained using the various schemes on the coarse grid. These plots exhibit trends similar to the previous test case. SOU and QUICK produced results with spurious oscillations, which were more pronounced with QUICK. The monotonic schemes noticeably improved the results. MSOU exactly captured the maximum field value, with the RMS error of its solution being the smallest among the solutions produced by the

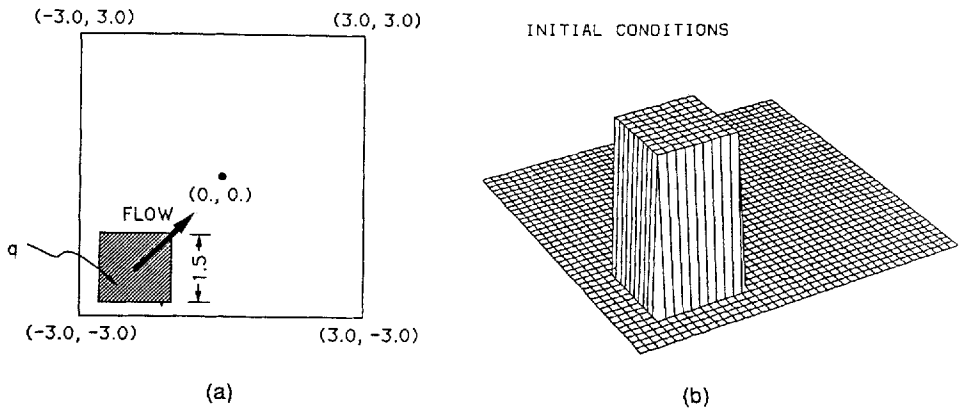

Figure 4. (a) Two-dimensional schematic of the 'square' scalar field test and (b) three-dimensional perspective of the initial scalar field

Table II. Performance of the various discretization schemes in the square-field transport test

	40 × 40 grid			80 × 80 grid		
Scheme	Max.	Min.	RMS error	Max.	Min.	RMS error
FOU	6·257	0·000	1·445	8·526	0·000	1·289
SOU	16·356	−3·580	1·268	18·880	−5·575	1·329
QUICK	18·808	−5·881	1·737	35·471	−21·092	3·366
MPL	9·973	0·000	0·936	10·000	0·000	0·717
MSOU	10·000	0·000	0·855	10·000	0·000	0·537
SHARP	10·219	−0·440	0·948	10·892	−1·373	0·652

various schemes on both grids. MPL also produced very good results, with 9 and 33% larger RMS errors than MSOU's, on the coarse and fine grids, respectively. SHARP performed less satisfactorily in this test problem, with its predictions being up to 21% less accurate than MSOU's on the fine grid. Also, SHARP failed to give oscillation-free results; small-magnitude oscillations, which were stronger than in the previous test case, persisted. Considering the quality of the results obtained by each scheme, MSOU is the most accurate scheme in this test problem.

Mixing of a hot with a cold front

This problem addresses the formation of cold and warm fronts in a two-dimensional setting. Beginning with a narrow region of high gradients (a front), a fixed (in time) rotational velocity field will act to twist the front in a manner similar to that observed on daily-weather maps.[29] The problem has the following analytical solution:

$$q(x, y, t) = -\tanh\left[\frac{y}{2}\cos(\omega t) - \frac{x}{2}\sin(\omega t)\right], \tag{26}$$

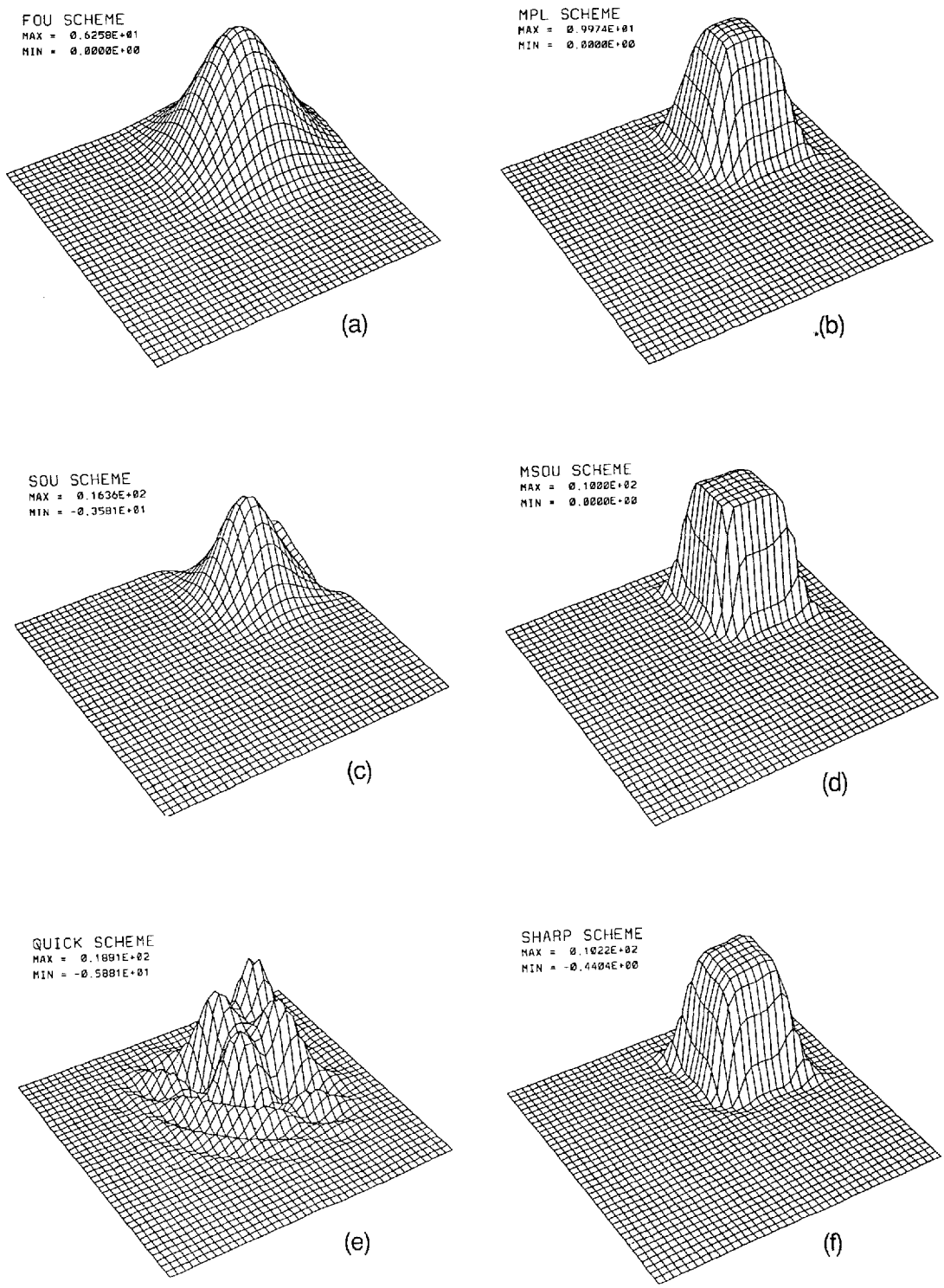

Figure 5. (a)–(f). Three-dimensional perspective plots of the solutions in the 'square' scalar field test

where $-4 \leqslant x \leqslant 4$, $-4 \leqslant y \leqslant 4$,

$$\omega = \frac{v_t}{r v_{t\,max}}, \tag{27}$$

ω being the frequency, $v_t = \mathrm{sech}^2(r)\tanh(r)$ is the tangential velocity around the centre, and $v_{t\,max}$ is the maximum tangential velocity, which is set equal to 0·385 for this problem. The initial conditions at $t=0$ are obtained from equation (26). Thus, the initial condition is a function of y only. The centre of the velocity field is at ($x=0$, $y=0$). The velocity components u and v are obtained using the following equations:

$$u(x, y) = -\frac{v_t}{v_{t\,max}}\frac{y}{r}, \tag{28}$$

$$v(x, y) = \frac{v_t}{v_{t\,max}}\frac{x}{r}. \tag{29}$$

The 2D plot of the initial scalar field, with the velocity field superimposed, is shown in Figure 6(a). The maximum and minimum values of the field were $q_{max} = 0{\cdot}964$ and $q_{min} = -0{\cdot}964$, respectively. Solid lines indicate positive values of the scalar variable, while dashed lines indicate negative values. The initial scalar field varies gradually from positive values at the bottom of Figure 6(a) to negative values at the top. Physically, positive values correspond to a warm front and negative values to a cold front. The flow field will twist the fronts and, after four time units, the exact analytical solution will be the one shown in Figure 6(b).

Five different grid sizes were used, starting from a 16×16 coarse grid and ending with a 256×256 fine grid. The RMS error of each scheme is shown in Table III as a function of grid size. Maximum and minimum values are not reported since no scheme introduced oscillations in the solution. Figures 7(a)–7(f) compare the calculated solutions from each scheme after four time units on the 32×32 grid. Clearly, the FOU solution shows the worst agreement with the

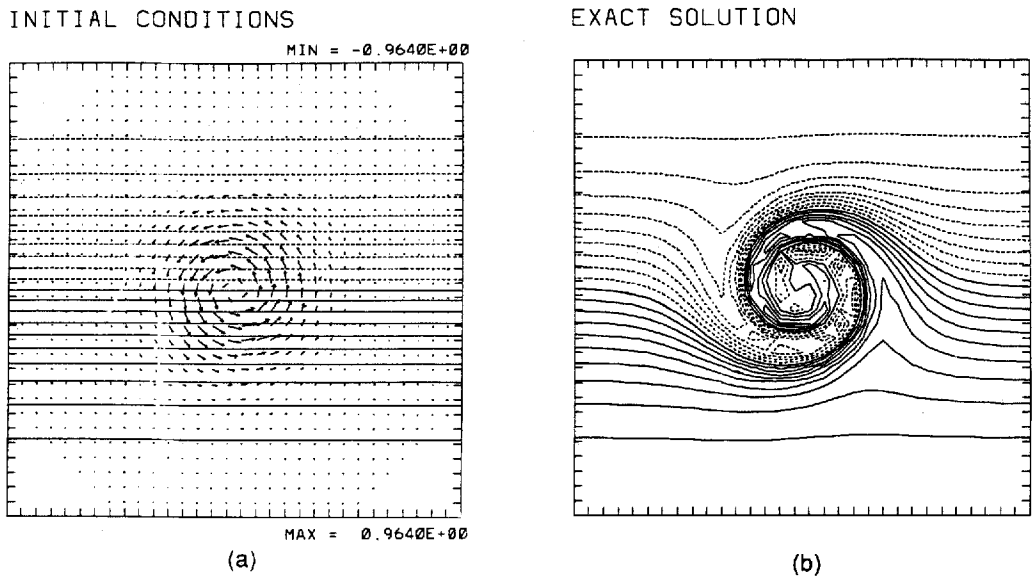

Figure 6. (a) Initial conditions in the mixing test and (b) exact analytical solution

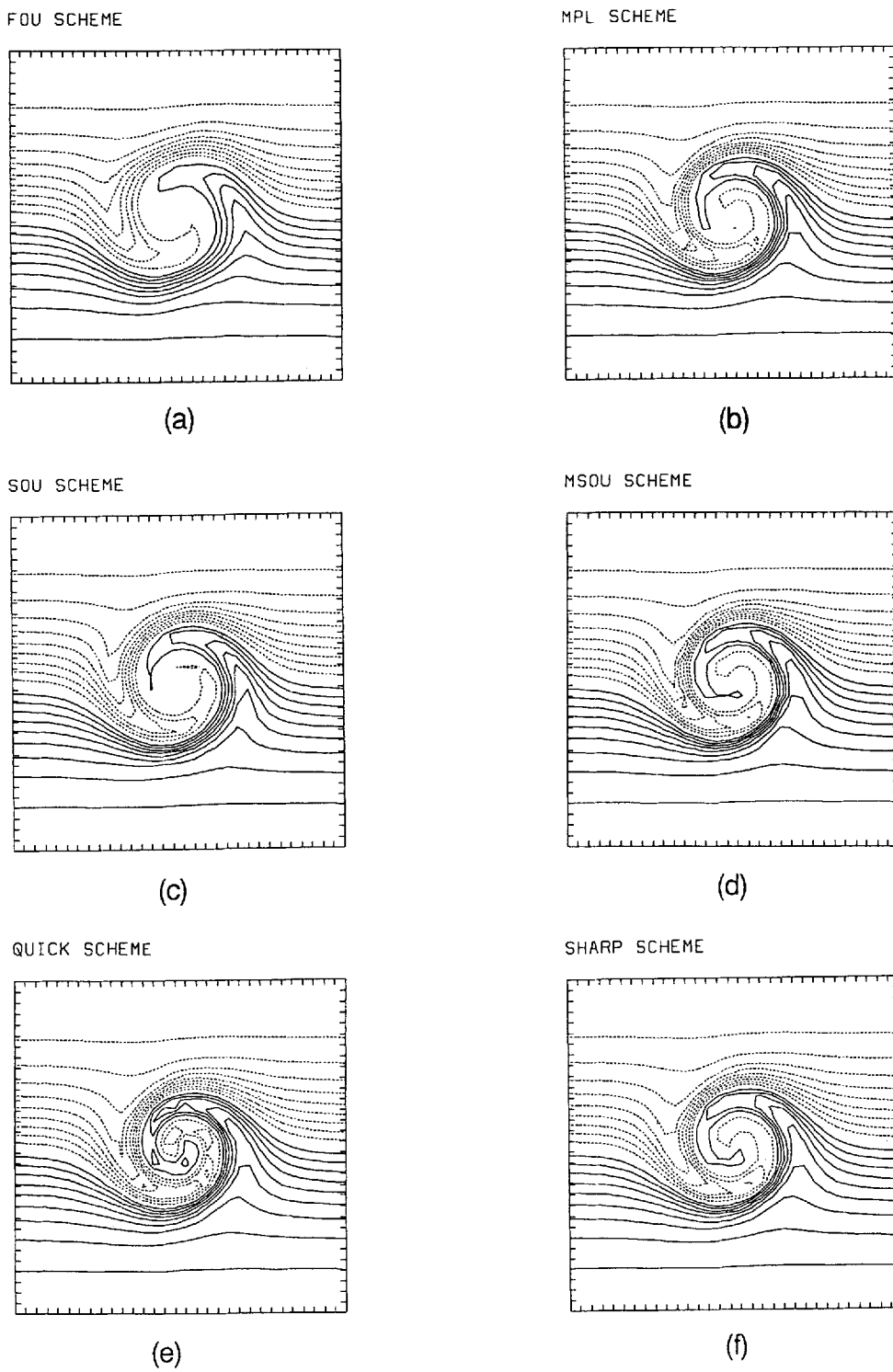

Figure 7(a)–(f). Contour plots of the scalar fields in the mixing test

Table III. RMS errors (× 100) of the various discretization schemes in the mixing test

Scheme	16 × 16	32 × 32	64 × 64	128 × 128	256 × 256
FOU	9·53	7·89	6·10	4·33	2·18
SOU	7·92	5·31	2·45	0·64	0·16
QUICK	6·70	3·96	1·23	0·32	0·08
MPL	7·00	4·70	2·18	1·05	0·54
MSOU	6·76	4·26	1·27	0·39	0·14
SHARP	6·65	4·28	1·58	0·40	0·10

analytical solution. The predictions improve by using higher-order schemes. As shown in Table III, the most accurate results are obtained by QUICK on all grids. SHARP gives somewhat less satisfactory results than QUICK. It is also found that MSOU improves the accuracy of the solution over SOU, by as much as 100% on a 64 × 64 grid, and as low as 14% on a 256 × 256 grid. Van Leer's MPL scheme gives less accurate results than its monotonic rivals, i.e. MSOU and SHARP.

Useful conclusions regarding the actual order of accuracy of each scheme can be drawn from Table III. This table is generated by reducing the size of the grid spacing by 50% from run to run, while keeping Δt constant, until the reduction in the RMS error exhibits a clear trend. The highest Courant number was approximately equal to 0.16 on the 256 × 256 grid. The fourfold reduction of the RMS error as the mesh interval is reduced by a factor of two (from a 128 × 128 to a 256 × 256 grid) shows that QUICK is actually a second-order scheme. On the other hand, the first-order accuracy of FOU and the second-order accuracy of SOU are verified. The monotonic schemes, which are strongly non-linear, do not follow their nominal order of accuracy. SHARP retains QUICK's second-order accuracy, MSOU approaches second-order accuracy and MPL behaves as a first-order scheme. Nevertheless, MPL is four times more accurate than the classical first-order FOU scheme. Overall, however, QUICK is the most satisfactory scheme for this problem.

Deformation of a cone-shaped scalar field

In the previous model problems, the schemes were evaluated in flow fields that were either uniform or smooth. In non-smooth or deformational flows, however, significant differences between schemes can be found, since the scheme monotonicity could depend on the structure of the velocity field. The deformational flow problem was initially defined by Smolarkiewicz.[10] In our version of this problem, a fixed (in time) flow field is defined by the stream function

$$\psi(x, y)=\frac{1}{4\pi}\sin[4\pi(x+0{\cdot}5)]\cos[4\pi(y+0{\cdot}5)]. \tag{30}$$

The domain is a square of side equal to one unit, and with the origin of the co-ordinate system located at its centre. Isolines of the stream function are shown in Figure 8(a), with the initial scalar distribution superimposed. The flow field consists of sets of symmetrical counterrotating vortices, as shown in Figure 8(b). Each vortex occupies a square of 0·25 units. The initial scalar distribution is a cone of radius 0·15 units, height equal to 1 unit, and it is centred at the origin of the co-ordinate system. The initial scalar distribution is non-zero over six vortices, and most of the cone's base area is included within the area of the two central vortices. Fluid elements are constrained to move along stream lines and, thus, cannot escape from the binding vortex in which

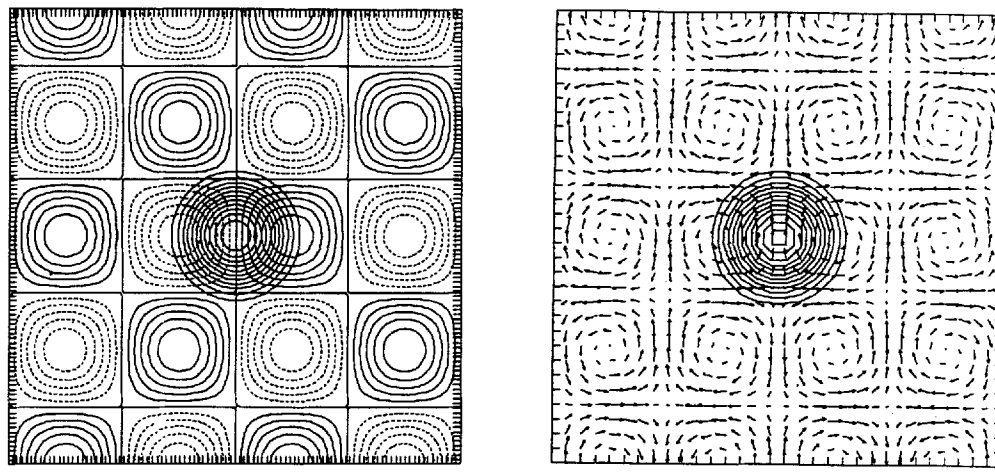

Figure 8. (a) Stream function contours and (b) velocity vectors in the deformation test. The initial scalar field is superimposed

Table IV. Performance of the various discretization schemes in the deformational flow problem

	100×100 grid		
Scheme	Max.	Min.	CPU ratio
FOU	0·127	0·000	1·00
SOU	0·199	−0·013	1·12
QUICK	0·226	−0·009	1·18
MPL	0·168	0·000	1·62
MSOU	0·200	0·000	1·50
SHARP	0·172	−0·000009	7·75

they are initially found. Therefore, at any time, the scalar distribution will be zero everywhere except in the six vortices where it is initially non-zero. One grid size consisting of 100×100 nodes has been used. The maximum Courant number was equal to 0·2 and the time integration consisted of 4000 iterations.

Figures 9(a)–9(f) illustrate the solution obtained using the various schemes. Solid lines indicate positive values of the scalar variable, while dashed lines indicate negative values. The maximum and minimum values are summarized in Table IV. Clearly, only the FOU, MPL and MSOU schemes predicted physically plausible solutions, where values of the scalar were restricted within the six central vortices. SOU and QUICK produced strong oscillations and overshoots, which resulted in non-zero scalar distributions over the entire domain. SHARP also failed to produce oscillation-free results, as seen in Figure 9(f). The MPL and MSOU results are comparable, with MSOU predicting somewhat steeper profiles.

The required computational effort associated with each scheme is shown in Table IV. The numbers have been non-dimensionalized with respect to the computer time required by the least

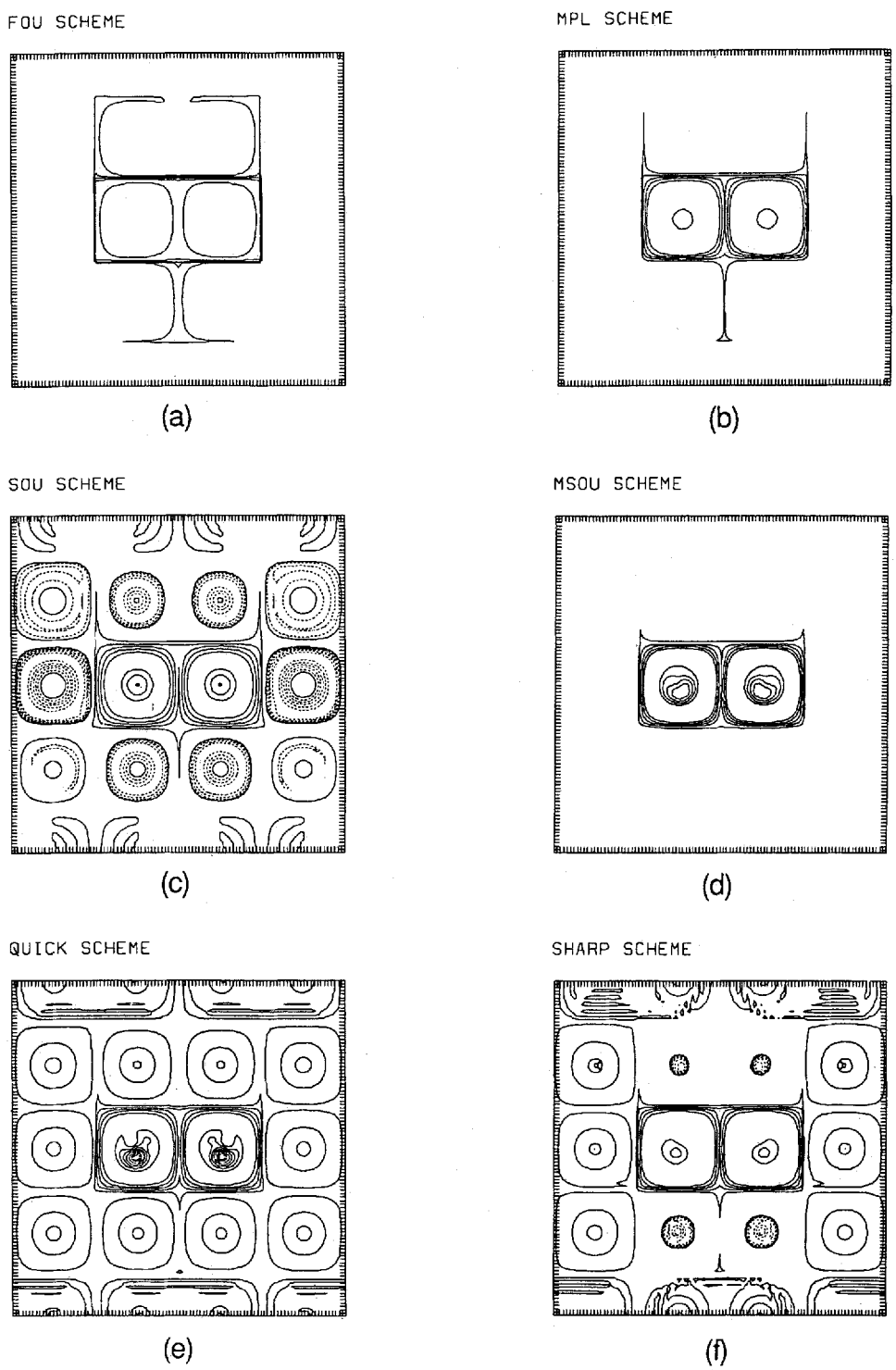

Figure 9. (a)–(f). Contour plots of the scalar fields in the deformation test

expensive FOU scheme. Apart from accuracy considerations, CPU results clearly prohibit SHARP's use since it requires about eight times more computer time than FOU. On the other hand, MSOU and MPL require about 50% more computer time than FOU, which makes them attractive choices, especially considering their accurate performance. SOU and QUICK consumed just about 15% more CPU time than FOU, but with poor results, as stated above. Based on accuracy and CPU considerations, MSOU is the clear winner in this test case.

CONCLUSIONS

Several high-order-accuracy schemes, with and without flux limiters, have been evaluated in four time-dependent, linear problems with pure convection. The predictive capabilities of each scheme have been assessed in terms of a number of sensible criteria. While the ultimate selection of a particular scheme should be based on the nature of a given problem, this work has produced the following guidelines for the selection process:

(i) The classical FOU scheme produces oscillation-free results but is very inaccurate, especially in problems involving steep gradients.

(ii) The SOU and QUICK schemes yield improved results for problems not involving discontinuous, or nearly discontinuous, profiles. Despite the finding that QUICK is actually second-order, it is more accurate than SOU. However, in problems where discontinuous profiles exist, QUICK introduces stronger oscillations than SOU.

(iii) Although MPL is found to be first-order, it improves considerably the accuracy of the solution in problems with discontinuous gradients of the advected variable. The small increase in its computer cost over FOU, along with its good accuracy, renders MPL a good choice for such problems.

(iv) MSOU's behaviour is nearly second-order in accuracy. Nevertheless, MSOU is the most accurate scheme in problems involving discontinuous gradients of the advected variable. Furthermore, taking into consideration its high computational efficiency, MSOU appears to be the best choice for problems with discontinuities.

(v) The SHARP scheme retains QUICK's second-order of accuracy. Although it allows small-amplitude oscillations in the solution of problems with discontinuous gradients, it can be very appropriate in flows where nearly continuous gradients exist. However, SHARP's high computational cost in vector machines, such as the Cray-Y/MP, could prohibit its usage in real-life applications.

ACKNOWLEDGEMENTS

This material is based upon work supported by the National Science Foundation under Grant No. CBT-8858310. The National Center for Supercomputing Applications at the University of Illinois at Urbana-Champaign provided computer time on the CRAY-Y/MP system for this study.

REFERENCES

1. J. N. Lillington, 'A vector upstream differencing scheme for problems in fluid flow involving significant source terms in steady-state linear systems', *Int. j. numer. methods fluids*, **1**, 3–16 (1981).
2. S. V. Patankar, *Numerical Heat Transfer and Fluid Flow*, Hemisphere, Washington, DC, 1980.
3. G. D. Raithby, 'Skew upstream differencing schemes for problems involving fluid flow', *Comput. methods appl. mech. eng.*, **9**, 153–164 (1976).
4. G. D. Raithby and K. E. Torrance, 'Upstream-weighted schemes and their application to elliptic problems involving fluid flow', *Comput. Fluids*, **2**, 191–206 (1974).

5. S. Syed, A. Gosman and M. Peric, 'Assessment of discretization schemes to reduce numerical diffusion in the calculation of complex flows', *Paper No. AIAA-85-0441*, 1985.
6. R. F. Warming and R. M. Beam, 'Upwind second-order difference schemes and applications in aerodynamic flows', *AIAA J.*, **14**, 1241–1249 (1976).
7. B. P. Leonard, 'A stable and accurate convective modeling procedure based on quadratic upstream interpolation', *Comput. methods appl. mech. eng.*, **19**, 59–98 (1979).
8. J. P. Boris and D. L. Book, 'Flux-corrected transport I: SHASTA, a fluid transport algorithm that works', *J. Comput. Phys.*, **11**, 38–69 (1973).
9. S. T. Zalesak, 'Fully multi-dimensional flux-corrected transport algorithms for fluids', *J. Comput. Phys.*, **31**, 335–362 (1979).
10. P. K. Smolarkiewicz, 'The multi-dimensional Crowley advection scheme', *Mon. Weather Rev.*, **110**, 1968–1983 (1982).
11. B. Van Leer, 'Towards the ultimate conservative difference scheme. IV. A new approach to numerical convection', *J. Comput. Phys.*, **23**, 276–299 (1977).
12. P. Colella and P. R. Woodward, 'The piecewise parabolic method (PPM) for gas–dynamical situations', *J. Comput. Phys.*, **54**, 174–201 (1984).
13. P. L. Roe, 'Approximate Riemann solvers, parameter vectors, and difference schemes', *J. Comput. Phys.*, **43**, 357–372 (1981).
14. P. L. Roe, 'Some contributions to the modeling of discontinuous flows', *Proc. AMS/SIAM Seminar*, San Diego, 1983.
15. S. R. Chakravarthy and S. Osher, 'A new class of high accuracy TVD schemes for hyperbolic conservation laws', *Paper No. AIAA-85-0363*, 1985.
16. A. Harten, 'High resolution schemes for hyperbolic conservation laws', *J. Comput. Phys.*, **49**, 375–393 (1983).
17. C. W. Shu and S. Osher, 'Efficient implementation of essentially non-oscillatory shock-capturing schemes', *J. Comput. Phys.*, **77**, 439–471 (1988).
18. C. W. Shu and S. Osher 'Efficient implementation of essentially non-oscillatory shock-capturing schemes, II', *J. Comput. Phys.*, **83**, 32–78 (1989).
19. H. Yang, 'An artificial compression method for ENO schemes: the slope modification method', *J. Comput. Phys.*, **89**, 125–160 (1990).
20. J. C. T. Wang and G. F. Windhopf, 'A high-resolution TVD finite volume scheme for the Euler equations in conservation form', *J. Comput. Phys.*, **84**, 145–173 (1989).
21. B. P. Leonard, 'Simple high-accuracy resolution program for convective modeling of discontinuities', *Int. j. numer. methods fluids*, **8**, 1291–1318 (1988).
22. P. H. Gaskell and A. K. C. Lau, Curvature compensated convective transport: SMART, a new boundedness preserving transport algorithm', *Int. j. numer. methods fluids*, **8**, 617–641 (1988).
23. P. K. Sweby, 'High resolution schemes using flux limiters for hyperbolic conservation laws', *SIAM J. Numer. Anal.*, **21**, 995–1001 (1984).
24. S. A. Orszag, 'Numerical simulation of incompressible flows within simple boundaries: accuracy', *J. Fluid Mech.*, **49**, 75–112 (1971).
25. P. Gresho, R. Lee and R. Sani, 'Advection-dominated flows-with emphasis on the consequences of mass lumping', in R. H. Gallagher, O. C. Zienkiewicz, J. T. Oden, M. Morandi, Cecchi and C. Taylor (eds), *Finite Elements in Fluids, Vol. 3*, Wiley, Chichester, 1978.
26. J. Donea and S. Guiliani, 'A simple method to generate high-order accurate convection operators for explicit schemes based on linear finite elements', *Int. j. numer. methods fluids*, **1**, 63–79 (1981).
27. W. D. Gropp, 'Local uniform mesh refinement with moving grids', *SIAM J. Sci. Stat. Comput.*, **49**, 357–393 (1983).
28. A. A. Amsden, P. J. O'Rourke and T. D. Butler, 'KIVA-II: A computer program for chemically reacting flows with sprays', *Los Alamos National Laboratory Report LA-11560-MS*, 1979.
29. C. A. Doswell, 'Kinematic analysis of frontogenesis associated with a nondivergent vortex', *J. Atmos. Sci.*, **41**, 1242–1248 (1984).